Available online at www.sciencedirect.com
SCIENCE DIRECT
International Journal of Heat and Mass Transfer 49 (2006) 3555–3560
International Journal of HEAT and MASS TRANSFER
www.elsevier.com/locate/ijhmt

# Average heat transfer rates measured in two different temperature ranges for magnetic convection of horizontal water layer heated from below

Azusa Ujihara [a], Toshio Tagawa [b], Hiroyuki Ozoe [c,*]

[a] Interdisciplinary Graduate School of Engineering Sciences, Kyushu University, Kasuga, Japan
[b] Department of Aerospace Engineering, Tokyo Metropolitan University, Asahigaoka 6-6, Hino, Tokyo 191-0065, Japan
[c] Faculty of Non-Ferrous Metals, AGH University of Science and Technology, Al. Mickiewicz 30, 30-059 Krakow, Poland

Received 21 July 2005
Available online 18 May 2006

**Abstract**

The average heat transfer rates of gravitational and magnetic convection of water heated from below and cooled from above are measured for two cases of cold wall temperature $\theta_c$ at 10 °C and 30 °C. The height of the cylindrical enclosure is 2 mm with 40 mm in diameter. The magnetic field is imposed in a vertical direction to increase or decrease 29% of the gravitational acceleration in a bore space of a super-conducting magnet of 10 T at the solenoid center. The group of data at $\theta_c = 30$ °C gives a better agreement with the classical heat transfer rate of Silveston than that at $\theta_c = 10$ °C. This is probably due to the almost constant value in the volumetric magnetic susceptibility of water at about 10 °C.


## 1. Introduction

At the beginning of 20th century, Bénard [1] took a photograph of hexagonal cell for the shallow layer of oil heated from below and cooled from free surface. This interesting picture inspired the theoretical work by Rayleigh [2] who defined the critical Rayleigh number, below which conductive heat transfer is dominant and over which convective heat transfer is a preferred mode. Then, extensive researches have been accumulated for the study of natural convection. This should be the reason why the natural convection of shallow layer heated from below and cooled from above has been called as the Rayleigh–Bénard problem. Recently, Braithwaite et al. [3] reported the enhanced and suppressed average heat transfer rates of Rayleigh–Bénard natural convection of gadolinium nitrate hexahydrate (paramagnetic fluid) in a strong gradient magnetic field. They employed a super-conducting magnet which provides magnetic (Kelvin) force for non-ferrous materials. This magnetic force could supply arbitrary magnitudes and orientation of acceleration for any materials in contrast to the uniform and constant value of gravitational acceleration. This means that this magnetic force may be employed as additional control force for any systems in addition to the gravitational acceleration force. Wakayama [4] reported a jet flow of nitrogen gas in a decreasing magnetic field as another example of this magnetic force. Bai et al. [5] made a numerical analysis for this, so to speak, Wakayama jet. Subsequently, Tagawa et al. [6] employed a similar way to Boussinesq approximation for this magnetic force and carried out numerical analysis for natural convection of air in a cubic enclosure. Kaneda et al. [7] studied that air in a cube heated from above and cooled from bottom is driven by a magnetic force. Maki et al. [8] studied the Rayleigh–Bénard convection of air in a magnetic field to support the magnetic Rayleigh number proposed by Braithwaite et al. [3]. Then, Tagawa et al. [9] studied the Rayleigh–Bénard natural convection of water computationally with the presumption that

* Corresponding author.
E-mail addresses: ttagawa@cc.tmit.ac.jp (T. Tagawa), ozoe@agh.edu.pl (H. Ozoe).

0017-9310/$ - see front matter © 2006 Elsevier Ltd. All rights reserved.
doi:10.1016/j.ijheatmasstransfer.2006.01.052

**Nomenclature**

| | | | |
|---|---|---|---|
| $A$ | heat transfer area ($m^2$) | $Ra$ | Rayleigh number $= g\beta(\theta_h - \theta_c)h^3/(\alpha\nu)$ (–) |
| AR | diameter of cylinder/height (–) | $Ra_m$ | $Ra[1-(\chi/(\mu_m g))(b_z\partial b_z/\partial z)]_{\text{at enclosure center}}$ (–) |
| $\vec{b}$ | magnetic induction vector ($T = kg\,s^{-2}\,A^{-1}$) | $z$ | axial coordinate (m) |
| $g$ | acceleration due to gravity ($m\,s^{-2}$) | | |
| $g'$ | $g[1-(\chi/(\mu_m g))(b_z\partial b_z/\partial z)]_{\text{at enclosure center}}$ ($m\,s^{-2}$) | *Greek symbols* | |
| $h$ | height of a cylindrical enclosure (m) | $\alpha$ | thermal diffusivity ($m^2\,s^{-1}$) |
| $i$ | electric current in a coil (A) | $\beta$ | volumetric coefficient of expansion ($K^{-1}$) |
| $k$ | thermal conductivity of water ($W\,m^{-1}\,K^{-1}$) | $\theta$ | temperature (°C) |
| $Nu$ | Nusselt number $= Q_{conv}/Q_{cond}$ (–) | $\theta_c$ | cold wall temperature (°C) |
| $Pr$ | Prandtl number $= \nu/\alpha$ (–) | $\theta_h$ | hot wall temperature (°C) |
| $Q$ | heat flux (W) | $\Delta\theta$ | $=\theta_h - \theta_c$ (°C) |
| $Q_{cond}$ | conduction heat flux (W) | $\mu_m$ | magnetic permeability ($H\,m^{-1}$) |
| $Q_{conv}$ | convection heat flux (W) | $\nu$ | kinematic viscosity ($m^2\,s^{-1}$) |
| $Q_{d\,tot}$ | total heat flux in conduction state (W) | $\rho$ | density ($kg\,m^{-3}$) |
| $Q_{loss}$ | heat loss (W) | $\chi$ | mass magnetic susceptibility ($m^3\,kg^{-1}$) |
| $Q_{v\,tot}$ | total heat flux in convection state (W) | $\chi_m$ | volumetric magnetic susceptibility $= \rho\chi$ (–) |

the water is a diamagnetic material, i.e., constant value in the mass magnetic susceptibility over a temperature change. By the way, Mogi et al. [10] reported that slight temperature dependence of mass magnetic susceptibility of water affects the natural convection in a levitated water droplet in a strong magnetic field at 20 T (Tesla = $kg\,s^{-2}\,A^{-1}$) or more. This problem was discussed at a recent meeting extensively [11]. Then, it would be worth to study if the above temperature dependence of mass magnetic susceptibility of water affects the classical Rayleigh–Bénard convection, since Rayleigh–Bénard convection is a basic system for the study of natural convection. In the present paper we study the average heat transfer rates of Rayleigh–Bénard magnetic convection of water measured in two different temperature ranges.

## 2. Experimental apparatus

Fig. 1 [11] shows $\chi(\theta)/\chi(20)$ and density $\rho(\theta)$ plotted versus temperature $\theta$ up to 60 °C. The mass magnetic susceptibility of water $\chi(\theta)$ changes about 1% over a wide range up to 80 °C or so. Furthermore the volumetric magnetic susceptibility $\chi_m(\theta) = \rho(\theta)\chi(\theta)$ is also plotted versus that at 20 °C, $\chi_m(20)$. $\chi_m(\theta)$ takes a maximum value at about 10 °C.

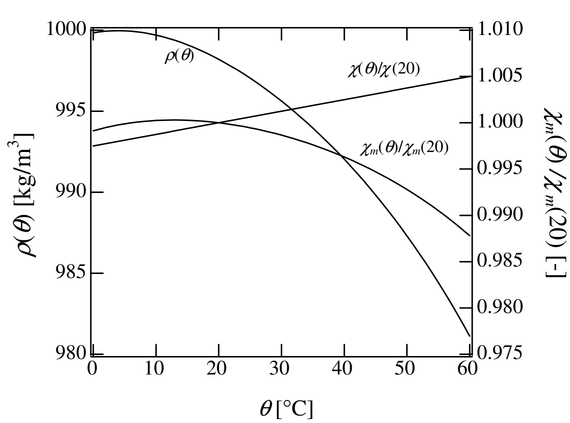


Fig. 1. Physical properties of water [10]. $\chi(\theta)$ is mass magnetic susceptibility $\chi_m(\theta)$ is volumetric magnetic susceptibility.

Fig. 2 shows a schematic view of the present experimental system. No. 1 shows a super-conducting magnet (HF10-100 VHT, Sumitomo Heavy Industry). An experimental cylinder is placed inside a bore of this magnet. No. 2 shows a constant temperature bath of water (CW301, Shibata) through which cooling water is circulated toward the experimental cylinder. No. 3 is a power supply of direct

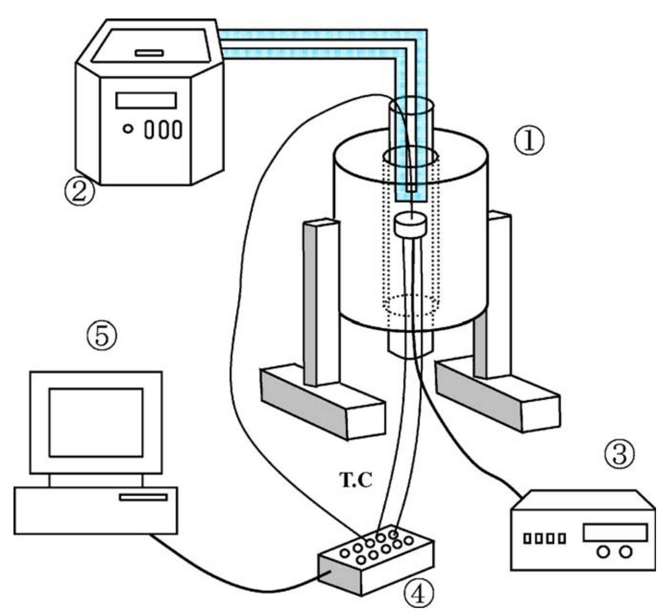


Fig. 2. Experimental set-up. (1) Super-conducting magnet; (2) constant temperature water bath; (3) power supply; (4) scanner for thermocouples; (5) personal computer.

current with constant voltage and current (PAN35-10A, Kikusui). No. 4 is a temperature measuring scanner (Jr. DC3100, NEC San-ei) connected to a number of thermocouples whose outputs are recorded in a personal computer (No. 5).

Fig. 3 shows a schematic view of the experimental apparatus located in a bore space of a super-conducting magnet. The center of the enclosure is placed at ±111 mm from the center of the magnetic coil whose axial length is ±0.064 m from the coil center. At these locations of ±111 mm, the radial component of magnetic force becomes minimum and we can expect to have mostly axial acceleration within the enclosure.

Fig. 4 shows a close-up view of the experimental apparatus. The experimental water is boiled, cooled and filled in a shallow cylindrical enclosure. The experimental water in it is cooled from an upper copper plate which is cooled by running water through a constant temperature bath. The lower copper plate is heated with Nichrome heater.

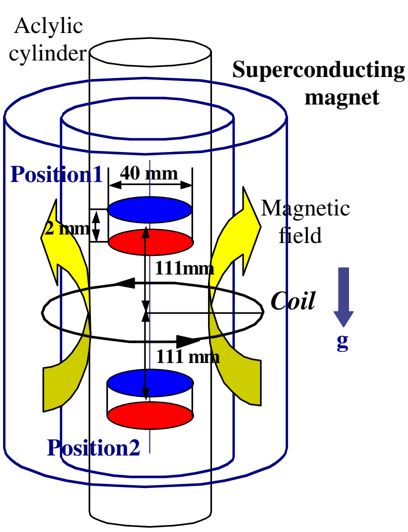


Fig. 3. Two locations for the experimental enclosure at positions 1 and 2.

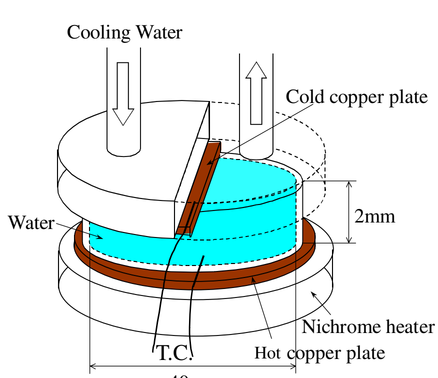


Fig. 4. Experimental apparatus for Rayleigh–Bénard natural convection of water.

The enclosure is 40 mm diameter with 2 mm thick. The vertical cylinder wall is prepared of 2 mm thick rubber sheet and 4 mm wide in a radial direction. This ratio $40/2 = 20 = \text{diameter/height}$ is expected to assure the wide shallow layer of Rayleigh–Bénard convection. The upper and lower copper plates are 3 mm thick in which about 1 mm diameter holes are drilled up to 3 mm and 12 mm deep from the center for a lower hot plate and 3 mm deep for an upper cold plate. T-type thermocouples are inserted in these holes.

## 3. Experimental procedure

In the present experiment, the net heat transfer rates are measured. For this we employ the procedure invented by Ozoe and Churchill [12]. At first, the cylindrical enclosure is placed upside-down to heat the water layer from the upper plate so that conduction heat transfer prevails. At various heating rates we could measure the temperature differences between the hot and cold walls. The net conduction heat flux through the water layer can be estimated by the Fourier law with known thermal conductivity of water for each temperature difference. Then we can obtain the data group between the total heat supply $Q$ [W] to the top plate versus the conduction temperature difference $\Delta\theta$ [K]. The heat loss $Q_{\text{loss}}$ can be given by

$$Q_{\text{loss}} = Q - kA\Delta\theta/h. \quad (1)$$

Fig. 5 shows the data schematically. The net conduction heat flux may be expressed as

$$Q_{\text{cond}} = Q - Q_{\text{loss}}. \quad (2)$$

Then we turn the enclosure as heated from below and repeat the convection experiments with several values of heat supply from the bottom plate. Presuming the heat loss

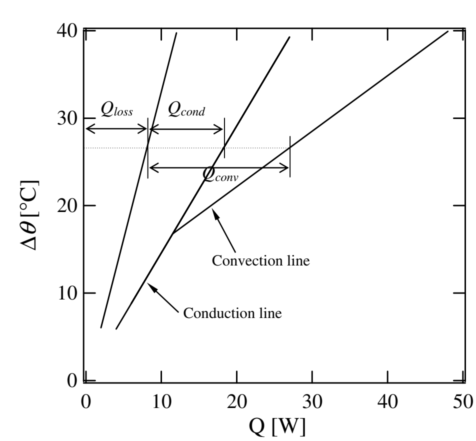


Fig. 5. Schematic drawings for the heat transfer measurement. $\Delta\theta$ is a temperature difference between the hot and cold plates and $Q$ is a total heat supply for the hot plate.

from the heater itself does not depend on the heat transfer states in an enclosure (conduction or convection) and we can estimate the net convection heat flux by using the $Q_{loss}$ curve of Eq. (1) for the corresponding temperature difference $\Delta\theta$,

$$Q_{conv} = Q - Q_{loss}. \quad (3)$$

These are shown in Fig. 5 in which we get the net convective heat flux $Q_{conv}$ and net conductive heat flux $Q_{cond}$ to give the average Nusselt number as follows.

$$Nu = Q_{conv}/Q_{cond}. \quad (4)$$

By the way, Braithwaite et al. [3] proposed the magnetic Rayleigh number as follows.

$$Ra_m = Ra[1 - (\chi/(\mu_m g))(b_z \partial b_z/\partial z)]_{\text{at enclosure center}}. \quad (5)$$

This is a summation of the gravitational Rayleigh number $Ra$ plus magnetic buoyancy equivalent. According to the examination table supplied from the manufacturer on the magnetic induction of the present magnet at 10 T at the solenoid center, $b_z \partial b_z/bz = \mp 390$ [T$^2$/m] at $z = \pm 111$ mm from coil center. Thus we can get the equivalent magnetic acceleration $g'$ as follows for $\chi = -9.07 \times 10^{-9}$ [m$^3$/kg] at temperature $\theta = 20$ °C.

$$\begin{aligned} g' &= g[1 - (\chi/(\mu_m g))(b_z \partial b_z/\partial z)] \\ &= 0.713 \text{ g at position 1 } (z = +111 \text{ mm}), \quad (6) \\ &= 1.287 \text{ g at position 2 } (z = -111 \text{ mm}). \quad (7) \end{aligned}$$

In this way, we can get about ±29% of the gravitational acceleration with the present 10 T magnet. Strictly the mass magnetic susceptibility is a function of temperature but it changes only 1% for 100 °C and the representative value at 20 °C is employed in computing $Ra_m$ in Eq. (5) in the subsequent results.

## 4. Experimental results

The temperature differences between the hot and cold plates are measured every 1 min for 100 min after steady states appear to have been reached.

The cooling temperature is set at 10 °C at the beginning. The preliminary experiments were carried out for the height of the cylinder enclosure 5 mm and 3.6 mm instead of 2 mm. The average Nusselt numbers are plotted versus $Ra_m$ as shown in Fig. 6(a) and (b). The experiments were carried out without and with the magnetic field at positions 1 and 2. The data are scattered erroneously for the height equal to 5 mm and much higher than the classical data by Silveston [13]. For the enclosure with the height equal to 3.6 mm, the data are rather lying together but much less than that of Silveston. The average

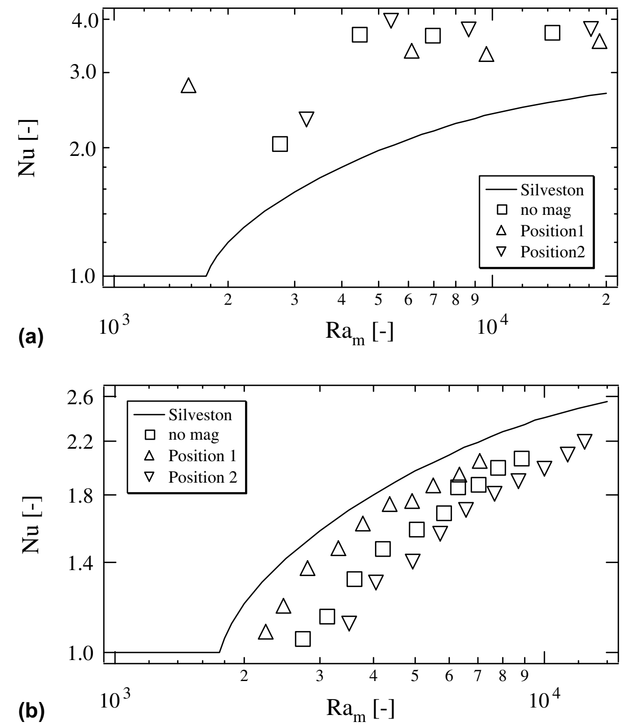


Fig. 6. Preliminary results for two enclosures of larger height. (a) 5 mm height and (b) 3.6 mm height.

heat transfer rates by Silveston and others are available in the book of Chandrasekhar [14] for the materials such as heptane, water, silicon oil AK3, ethylene glycol, air and silicon oil AK350. These data have been considered to be quite reliable for the Rayleigh–Bénard natural convection. We presumed our erroneous results for the heights of enclosure of 5 mm and 3.6 mm are due to the inaccuracy in measuring the temperature difference between the hot and cold plates at these ranges of the Rayleigh number. Thus we tried the height of 2 mm for the following reasons. Since the Rayleigh number is proportional to the cubic order of the representative length, i.e., height of the enclosure $h$ in the present case, the temperature difference for the same Rayleigh number differs extensively for

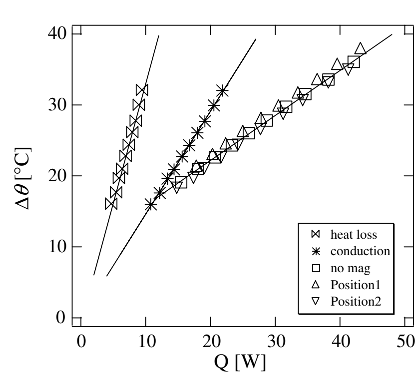


Fig. 7. Experimental results for 2 mm height enclosure at $\theta_c = 10$ °C.

Table 1
Experimental results at $\theta_c = 10$ °C

| $\Delta\theta$ [°C] | $Q_{d\,tot}$ | $Q_{cond}$ | $Q_{loss}$ |
|---|---|---|---|
| *(a) Conduction* | | | |
| 16.00 | 10.80 | 6.02 | 4.781 |
| 17.60 | 12.17 | 6.64 | 5.535 |
| 19.61 | 13.37 | 7.41 | 5.956 |
| 20.92 | 14.38 | 7.92 | 6.456 |
| 22.73 | 15.63 | 8.63 | 7.000 |
| 24.31 | 16.73 | 9.25 | 7.478 |
| 26.07 | 17.97 | 9.95 | 8.024 |
| 27.69 | 19.14 | 10.59 | 8.553 |
| 29.94 | 20.52 | 11.48 | 9.037 |
| 32.02 | 21.83 | 12.32 | 9.512 |

| $\Delta\theta$ [°C] | $Q_{v\,tot}$ | $Q_{conv}$ | $Q_{cond}$ | $Nu$ | $Ra$ |
|---|---|---|---|---|---|
| *(b) Natural convection* | | | | | |
| 19.10 | 15.48 | 9.61 | 7.22 | 1.331 | 2088 |
| 20.98 | 18.07 | 11.64 | 7.96 | 1.463 | 2460 |
| 22.61 | 20.69 | 13.78 | 8.60 | 1.602 | 2791 |
| 24.31 | 23.30 | 15.88 | 9.26 | 1.714 | 3172 |
| 26.02 | 25.94 | 18.02 | 9.93 | 1.813 | 3595 |
| 27.80 | 28.70 | 20.25 | 10.63 | 1.904 | 4082 |
| 29.75 | 31.68 | 22.65 | 11.40 | 1.987 | 4642 |
| 31.53 | 34.65 | 25.09 | 12.09 | 2.075 | 5196 |
| 33.58 | 38.21 | 28.04 | 12.90 | 2.174 | 5859 |
| 36.08 | 42.11 | 31.20 | 13.88 | 2.248 | 6784 |

| $\Delta\theta$ [°C] | $Q_{v\,tot}$ | $Q_{conv}$ | $Q_{cond}$ | $Nu$ | $Ra$ | $Ra_m$ |
|---|---|---|---|---|---|---|
| *(c) Magnetic convection at position 1* | | | | | | |
| 21.34 | 17.91 | 11.37 | 8.10 | 1.404 | 2517 | 1796 |
| 23.01 | 20.41 | 13.38 | 8.75 | 1.528 | 2867 | 2045 |
| 24.51 | 22.44 | 14.96 | 9.34 | 1.602 | 3222 | 2298 |
| 26.25 | 25.09 | 17.10 | 10.02 | 1.706 | 3630 | 2590 |
| 28.11 | 27.88 | 19.34 | 10.75 | 1.798 | 4116 | 2936 |
| 29.83 | 30.6 | 21.54 | 11.43 | 1.885 | 4620 | 3296 |
| 31.67 | 33.59 | 23.99 | 12.15 | 1.974 | 5186 | 3700 |
| 33.56 | 36.56 | 26.40 | 12.89 | 2.048 | 5813 | 4147 |
| 35.71 | 39.65 | 28.85 | 13.73 | 2.101 | 6626 | 4727 |
| 37.94 | 43.25 | 31.79 | 14.61 | 2.176 | 7467 | 5327 |
| 40.18 | 47.09 | 34.96 | 15.49 | 2.258 | 8406 | 5997 |

| $\Delta\theta$ [°C] | $Q_{v\,tot}$ | $Q_{conv}$ | $Q_{cond}$ | $Nu$ | $Ra$ | $Ra_m$ |
|---|---|---|---|---|---|---|
| *(d) Magnetic convection at position 2* | | | | | | |
| 18.24 | 14.88 | 9.26 | 6.88 | 1.346 | 1915 | 2464 |
| 19.64 | 17.46 | 11.43 | 7.43 | 1.537 | 2198 | 2829 |
| 21.00 | 19.14 | 12.70 | 7.97 | 1.595 | 2464 | 3170 |
| 22.52 | 21.71 | 14.82 | 8.56 | 1.731 | 2783 | 3581 |
| 24.30 | 24.32 | 16.91 | 9.26 | 1.826 | 3182 | 4093 |
| 26.52 | 27.81 | 19.74 | 10.13 | 1.948 | 3737 | 4808 |
| 28.68 | 31.32 | 22.61 | 10.98 | 2.059 | 4309 | 5544 |
| 30.60 | 34.34 | 25.06 | 11.73 | 2.136 | 4874 | 6270 |
| 33.10 | 38.29 | 28.26 | 12.71 | 2.224 | 5692 | 7323 |
| 34.90 | 41.37 | 30.81 | 13.42 | 2.297 | 6338 | 8155 |

different heights. For the same value of the Rayleigh number, temperature difference $\Delta\theta = 10$ °C for $h = 2$ mm becomes $\Delta\theta = 0.64$ °C for $h = 5$ mm, since $10 \times 2^3 = \Delta\theta \times 5^3$. The measurement for temperature difference of the order of $\Delta\theta = 10$ °C for $h = 2$ mm becomes $\Delta\theta = 0.64$ °C for $h = 5$ mm which becomes much inaccurate.

Fig. 7 shows the bare data of temperature difference $\Delta\theta$ [°C] versus the heat supply to the hot plate $Q$ [W] at the cold wall kept at 10 °C. These data are listed in Table 1 for (a) conduction, (b) convection without a magnetic field, (c) convection at position 1 and (d) at position 2, respectively. These are plotted in Fig. 8, (a) for $Nu$ versus $Ra_m$. Three sets of data agree well with the classical experimental data by Silveston. However, even with using the magnetic Rayleigh number, some scatter in the data appears to occur especially for the data obtained at position 1. At position 1, the magnetic force cancels the gravitational acceleration about 30% and the net acceleration is less than that of terrestrial state. The data at position 1 for 0.713 g appear to differ more from those of Silveston than those at position 2 for 1.287 g. Probably this is because the convection strength at weaker acceleration should be weaker and less definitive.

Since the temperature range at about 10 °C appears to give almost constant value in the volume magnetic susceptibility as seen in Fig. 1, we then tried to carry another run of experiment with keeping the cold wall temperature at 30 °C as follows.

Table 2 shows the corresponding data for the cold wall temperature at 30 °C. Fig. 8(b) shows these plots, for $Nu$ versus $Ra_m$. The data appear to be better correlated than Fig. 8(a) to suggest that the magnetic force is better correlated for the data at $\theta_c = 30$ °C than those at $\theta_c = 10$ °C. This is because as seen in Fig. 1, the volumetric magnetic susceptibility changes with temperature at about 30 °C and the magnetic buoyant force should be well represented by the magnetic Rayleigh number.

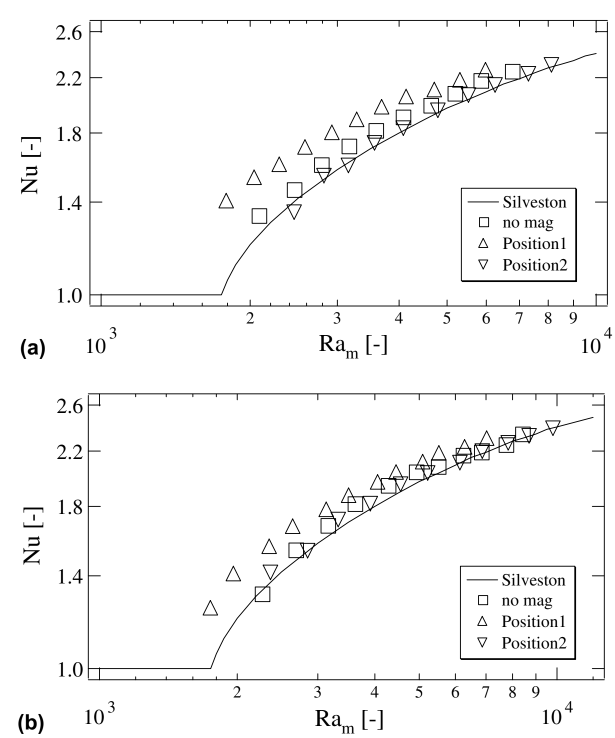


Fig. 8. Experimental results at (a) $\theta_c = 10$ °C and (b) $\theta_c = 30$ °C.

Table 2
Experimental results at $\theta_c = 30$ °C

| $\Delta\theta$ [°C] | $Q_{d\,tot}$ | $Q_{cond}$ | $Q_{loss}$ |
|---|---|---|---|
| *(a) Conduction* | | | |
| 12.87 | 9.42 | 5.06 | 4.36 |
| 16.56 | 11.95 | 6.54 | 5.41 |
| 20.52 | 14.74 | 8.14 | 6.60 |
| 23.48 | 16.90 | 9.34 | 7.56 |
| 26.76 | 19.26 | 10.68 | 8.58 |
| 30.94 | 22.39 | 12.39 | 10.00 |

| $\Delta\theta$ [°C] | $Q_{v\,tot}$ | $Q_{conv}$ | $Q_{cond}$ | $Nu$ | $Ra$ |
|---|---|---|---|---|---|
| *(b) Natural convection* | | | | | |
| 9.72 | 8.23 | 4.94 | 3.78 | 1.309 | 2272 |
| 11.17 | 10.44 | 6.70 | 4.36 | 1.535 | 2692 |
| 12.70 | 12.58 | 8.36 | 4.98 | 1.678 | 3165 |
| 14.06 | 14.69 | 10.04 | 5.53 | 1.815 | 3627 |
| 15.93 | 17.44 | 12.21 | 6.29 | 1.940 | 4286 |
| 17.60 | 19.95 | 14.20 | 6.97 | 2.037 | 4936 |
| 19.05 | 21.90 | 15.69 | 7.56 | 2.077 | 5514 |
| 20.75 | 24.58 | 17.84 | 8.25 | 2.164 | 6249 |
| 22.26 | 26.60 | 19.39 | 8.86 | 2.189 | 6853 |
| 24.18 | 29.47 | 21.66 | 9.64 | 2.248 | 7758 |
| 25.64 | 32.18 | 23.91 | 10.23 | 2.338 | 8428 |

| $\Delta\theta$ [°C] | $Q_{v\,tot}$ | $Q_{conv}$ | $Q_{cond}$ | $Nu$ | $Ra$ | $Ra_m$ |
|---|---|---|---|---|---|---|
| *(c) Magnetic convection at position 1* | | | | | | |
| 10.44 | 8.57 | 5.06 | 4.07 | 1.243 | 2460 | 1755 |
| 11.44 | 10.12 | 6.29 | 4.47 | 1.407 | 2761 | 1969 |
| 13.18 | 12.41 | 8.04 | 5.18 | 1.553 | 3307 | 2359 |
| 14.38 | 14.21 | 9.46 | 5.66 | 1.671 | 3723 | 2656 |
| 16.31 | 16.80 | 11.45 | 6.45 | 1.776 | 4407 | 3144 |
| 17.64 | 18.82 | 13.06 | 6.99 | 1.869 | 4933 | 3519 |
| 19.56 | 21.60 | 15.23 | 7.76 | 1.962 | 5706 | 4071 |
| 20.95 | 23.74 | 16.94 | 8.33 | 2.034 | 6265 | 4469 |
| 23.01 | 26.79 | 19.35 | 9.16 | 2.112 | 7159 | 5107 |
| 24.36 | 29.02 | 21.15 | 9.71 | 2.179 | 7766 | 5540 |
| 26.54 | 32.15 | 23.60 | 10.59 | 2.228 | 8841 | 6307 |
| 28.54 | 35.40 | 26.23 | 11.40 | 2.300 | 9883 | 7050 |

| $\Delta\theta$ [°C] | $Q_{v\,tot}$ | $Q_{conv}$ | $Q_{cond}$ | $Nu$ | $Ra$ | $Ra_m$ |
|---|---|---|---|---|---|---|
| *(d) Magnetic convection at position 2* | | | | | | |
| 8.26 | 7.33 | 4.50 | 3.18 | 1.413 | 1846 | 2375 |
| 9.60 | 8.95 | 5.70 | 3.73 | 1.529 | 2224 | 2861 |
| 10.91 | 10.95 | 7.29 | 4.26 | 1.712 | 2595 | 3339 |
| 12.33 | 12.87 | 8.76 | 4.83 | 1.813 | 3051 | 3925 |
| 13.90 | 15.24 | 10.64 | 5.47 | 1.946 | 3554 | 4573 |
| 15.40 | 17.38 | 12.32 | 6.08 | 2.026 | 4072 | 5239 |
| 17.25 | 20.01 | 14.37 | 6.83 | 2.104 | 4788 | 6161 |
| 18.67 | 22.33 | 16.24 | 7.40 | 2.194 | 5359 | 6895 |
| 20.51 | 25.09 | 18.43 | 8.15 | 2.261 | 6109 | 7860 |
| 22.09 | 27.53 | 20.37 | 8.79 | 2.318 | 6787 | 8732 |
| 24.03 | 30.59 | 22.83 | 9.58 | 2.384 | 7651 | 9843 |

## 5. Conclusion

The average Nusselt numbers are measured for the gravitational and magnetic convection of water for the cooling wall temperature $\theta_c = 10$ °C and 30 °C in the bore space of a super-conducting magnet of 10 T at the solenoid center. The experimental apparatus is placed at ±111 mm from a coil center to have 29% smaller or larger gravitational acceleration. The average Nusselt numbers measured for these sets agree approximately with the Silveston's data when plotted versus the magnetic Rayleigh number proposed by Braithwaite et al. However the average Nusselt number for $\theta_c = 10$ °C gave slightly more scattered than those for $\theta_c = 30$ °C when they are plotted versus the magnetic Rayleigh numbers as shown in the graph and tabulated values. This suggests that the anomalous temperature dependence of volumetric magnetic susceptibility of water at about 10 °C may not be simply expressed with magnetic Rayleigh number. However, the present experimental data are expected to be useful to compare with the subsequent theoretical works.

## References


[1] H. Bénard, Les Tourbillons cellulaires dans une nappe liquide, Revue gencrale des Sciences pures et appliqués 11 (1900) 1261–1271, and 1309–1328.

[2] L. Rayleigh, On convective currents in a horizontal layer of fluid when the higher temperature is on the under side, Philos. Mag. 32 (1916) 529–546.

[3] D. Braithwaite, E. Beaugnon, R. Tournier, Magnetically controlled convection in a paramagnetic fluid, Nature (London) 354 (1991) 134–136.

[4] N.I. Wakayama, Behavior of flow under gradient magnetic field, J. Appl. Phys. 69 (4) (1991) 2734–2736.

[5] B. Bai, A. Yabe, J. Qi, N.I. Wakayama, Quantitative analysis of air convection caused by magnetic–fluid coupling, AIAA J. 37 (12) (1999) 1538–1543.

[6] T. Tagawa, R. Shigemitsu, H. Ozoe, Magnetizing force modeled and numerically solved for natural convection of air in a cubic enclosure: effect of the direction of the magnetic field, Int. J. Heat Mass Transfer 45 (2002) 267–277.

[7] M. Kaneda, T. Tagawa, H. Ozoe, Convection induced by a cusp-shaped magnetic field for air in a cube heated from above and cooled from below, J. Heat Transfer 124 (2002) 17–25.

[8] S. Maki, T. Tagawa, H. Ozoe, Enhanced convection or quasi-conduction states measured in a super-conducting magnet for air in a vertical cylindrical enclosure heated from below and cooled from above in a gravity field, J. Heat Transfer 124 (2002) 668–673.

[9] T. Tagawa, A. Ujihara, H. Ozoe, Numerical computation for Rayleigh-Bénard convection of water in a magnetic field, Int. J. Heat Mass Transfer 46 (2003) 4097–4104.

[10] I. Mogi, C. Umeki, K. Takahashi, S. Awaji, K. Watanabe, M. Motokawa, Control of thermal convection in water by strong gradient magnetic fields, Jpn. J. Appl. Phys. 42 (2003) L715–L717.

[11] M. Yamaguchi, Chairman, The second meeting of the research project on the Development of New Functions of Strong Magnetic Field, Do water and magnetic field affect each other? Matsumoto, July 9–10, 2004.

[12] H. Ozoe, S.W. Churchill, Hydrodynamic stability and natural convection in Newtonian and non-Newtonian fluids heated from below, AIChE Symp. Ser. 69 (131) (1973) 126–133.

[13] P.L. Silveston, Wämedurchgang in waagerechten Flussigkeitsschichten, Part 1, Forsch. Ing. Wes. 24 (1958) 29–32, and 59–69.

[14] S. Chandrasekhar, Hydrodynamic and Hydromagnetic Stability, Dover Pub. Inc., 1961, p. 68.